Assistive Robotic Hand Orthosis (ARHO) controlled with EMG: evaluation of a preliminary prototype*

Diogo Farinha, João Dias, Pedro Neves, Kátia Pereira, Carlos Ferreira, Gabriel Pires

***Abstract*— Hand impairment severely limits basic activities of daily living (ADL). The use of motorized hand orthoses may provide enough functional assistance to perform basic tasks, such as grasping objects. Several prototypes have been proposed in the last decade, but there are still no solutions with the desired features regarding the weight, wearability and functionality. This paper describes the overall implementation of a prototype of an assistive robotic hand orthosis (ARHO) for object grasping, that can be triggered manually or by the detection of muscular activity in the forearm using surface electromyography (sEMG). The system is being specifically designed for a case study of a person with hemiplegia resulting from a peri-insular hemispherectomy. The proposed orthosis is a very preliminary but functional prototype, still far from the desired features mentioned above, but serves to show all the modules composing a low-cost implementation, and above all, to understand all the constraints and difficulties in designing such a system.**

I. INTRODUCTION

There are numerous diseases and events that cause motor disability and require rehabilitation treatment based on physiotherapy and occupational therapy. The use of robotic rehabilitation systems represents today an important complement to conventional therapy systems due to the advantage of performing repetitive movements with high intensity and precision. They can serve a greater number of patients because they are highly customizable, meeting the needs of each patient [1], and can also be used to quantify the therapy progress [2]. In cases where movement recovery is not possible, the development of robotic assistance systems, such as exoskeletons, can help in the replacement of lost functionalities in the affected members, assisting users in daily living activities. While a rehabilitation device is to be used in a rehabilitation center or at home with only the minimum usability requirements, an assistive device is used in daily activities, and should comply with extremely important usability aspects such as comfort, ergonomics, ease of use, functionality, autonomy and aesthetics.

Several prototypes of hand-assistive exoskeletons/orthoses have been proposed in the last decades (see an extensive survey in [3]). Successful approaches have been presented following rigid-frame [4], semi-rigid [5] and soft [6] designs. In [4], a wearable multi-phalangeal orthosis was designed to allow for a functional and safe interaction with the user's hand and to minimize the human-orthosis rotational axes misalignment. In [5], the hand exoskeleton is a glove with cables connected to the fingertips and a set of servomotors that are in a backpack. The system can be controlled using a switch with preprogrammed positions or by EMG. The glove was made in Spandex, a material with high flexibility. The guide rails to hold and maintain the cables centered on each finger were made in three-dimensional printing plastic. These cables are mounted on a Bowden system to enable power transmission between the fingers and the servomotors. In [6], an exo-glove was designed based on a soft tendon routing system inspired in the human musculoskeletal system. The exo-glove was designed for operation without pre-tensioning, which resulted in improved safety and comfort. Although important advances and encouraging results have been achieved even with motor impaired participants, systems still suffer from several limitations that hamper their acceptance by users. Some reported issues are related to systems' high costs, high complexity, low usability, lack of palm and fingers somatosensation, and systems' unfeasibility for some motor impairment situations, such as high spasticity.

This paper describes the development phases of a low-cost prototype of a rigid hand exoskeleton called ARHO (Assistive Robotic Hand Orthosis) that enables grasping motion. It can be triggered manually or automatically by detecting movement intention through sEMG. The prototype is being designed as a case study for assistance of a person with hemiplegia and high spasticity resulting from a peri-insular hemispherectomy. The several steps of the prototype development are described, covering the mechanical design, actuation, EMG signal processing and 3D modelling of the hand customized to the hemiplegic participant. Experimental tests were performed by 3 healthy participants and the hemiplegic participant.

II. METHODS

A. ARHO prototype

The ARHO prototype and respective functional diagram are illustrated respectively in Fig.1 and Fig.2. The system can be divided into 5 functional blocks: signal acquisition, signal processing, position control of linear motors, motors' power

*This work has been financially supported by the Project B-RELIABLE: PTDC/EEI-AUT/30935/2017 and the Project EXOBIKE: SAICT-POL/24013/2016 with FEDER/FNR/OE funding through programs CENTRO2020 and FCT.

Diogo Farinha is with the Polytechnic Institute of Tomar, 2300-313 Tomar, Portugal (e-mail: diogo_farinha@outlook.com).

João Dias is with the Polytechnic Institute of Tomar, 2300-313 Tomar, Portugal (e-mail: joaopdias@ipt.pt).

Pedro Neves is with the Polytechnic Institute of Tomar, 2300-313 Tomar, Portugal (e-mail: pedroneves@ipt.pt).

Kátia Pereira is with the Clinic4you, 3040-373 Coimbra Portugal (e-mail: katia_p.rr@hotmail.com)

Carlos Ferreira, IEEE Member, is with the Polytechnic Institute of Tomar, 2300-313 Tomar, Portugal (e-mail: cferreira@ipt.pt)

Gabriel Pires, IEEE Member, is with the Polytechnic Institute of Tomar, 2300-313 Tomar, and also with the Institute of Systems and Robotics, University of Coimbra, 3030-290 Coimbra, Portugal (corresponding author e-mail: gppires@ipt.pt).

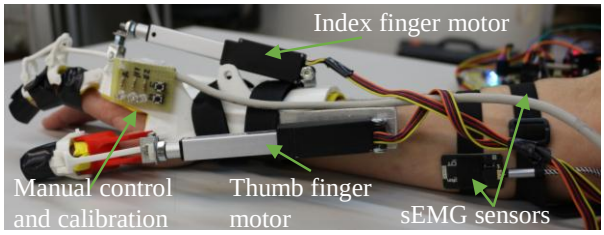

Figure 1. Picture of ARHO during an experiment.

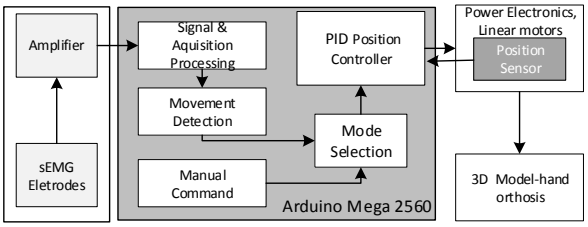

Figure 2. System functional diagram.

drive, and 3D modeled exoskeleton. The biosignal acquisition is based on two analog sEMG sensors (Gravity, Oymotion). The entire process of EMG signal sampling and processing, as well as control of the motors is done in an Arduino Mega 2560. The actuators are two Firgelli L16-50-35-12-P linear motors [7], one coupled to the index finger and the other to the thumb. A customized power driver was designed for this specific application. The system has three modes of operation, namely, the manual mode, the EMG-triggered mode and the EMG-controlled mode. In manual mode, the user can control the hand orthosis through a button, for example using the non-affected hand. In the EMG-triggered mode, a full movement of opening/closing is performed if the muscular activity exceeds a threshold at a given instant. In the controlled-EMG mode, to maintain the open/close movement, the muscular activity must be always above a threshold value. The main parts of the system are described below. The configuration, calibration and selection of operation modes can be set in the control pad buttons. The LEDs indicate the status.

B. *Power drive actuation and control*

The ARHO has two linear motors to control the index and thumb fingers to achieve pinch movements, but the mechanical design of ARHO allows to grasp objects. Although the Firgelli motors are commonly used by the research community and in commercial systems, for the best of our knowledge, no one has provided until now its transfer function. Therefore, the first step was to obtain the voltage-to-speed transfer function, considering a 1st order model. The procedure is not straightforward since the motor only provides position sensing. After applying a step voltage function, the response was differentiated and fitted with a 2nd order polynomial to eliminate noise. The gain and time constants obtained were respectively k_m=*3.75* and T_m= *0.0271* s, i.e., the voltage to position transfer function is given by

$$G(s) = \frac{138.3}{s^2 + 36.89s} \qquad (1)$$

The motors are controlled in position with a PID controller, which was tuned in continuous-time using the Matlab™ *pidTuner* function. Then it was converted into digital by applying backward difference to the derivative component and Tustin's approximation to the integral component. The difference equation of the digital controller is given by

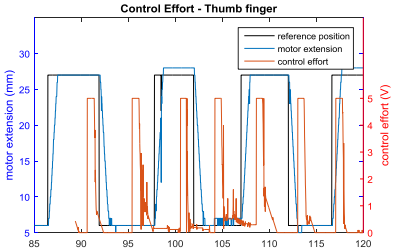

Figure 3. Position output and controller command, resulting from u(k), of thumb finger motor for step references.

$$u(k) = b_0.e(k) - b_1.e(k-1) + b_2.e(k-2) + u(k-1) \qquad (2)$$

where b_0, b_1 and b_2 are the control coefficients given respectively by *8.664*, *-14.788* and *6.129*, *e(k)* is the position error (difference between the reference value and the motor position), and *u(k)* is the PID output. This output is then mapped into a PWM command that actuates the power converter, composed of a double bridge converter L293 that actuates the two motors. Fig. 3 shows the control command of the thumb finger motor and the controller output *u(k)* for step references. This module together with the Arduino platform and the batteries are held in a lateral pocket worn by the user. ARHO allows the parameterization of values such as the opening/closing limits, individual motor speed, switching between control modes, and setting the EMG's thresholds.

C. *EMG signal acquisition and processing*

The signal processing pipeline comprises: 1) pre-processing, where filters are applied to eliminate the unwanted frequencies, noise and artifacts; 2) baseline correction; 3) buffering/windowing; 4) feature extraction; and 5) intention detection. The EMG processing pipeline was a customized solution to ensure its implementation in the low-computation microcontroller, which is also responsible for motor control.

The EMG signals were recorded from the *flexor carpi ulnaris* and the *extensor carpi Radialis* in the participants forearm following a bipolar montage. The sampling frequency was set to 250 Hz, considering the microcontroller processing power and memory capacity. The signal was filtered with a 4th IIR Butterworth band pass filter with cutoff frequencies 20 Hz and 100 Hz. The 20 Hz cutoff frequency eliminated artifacts derived from arm movements and other unwanted movements of the electrodes or body. Two Notch filters at 50 Hz and 100 Hz were also implemented to eliminate the noise produced by the electrical network. All filters were implemented in the Direct Form II realization.

EMG signals are buffered in windows (segments) of 1 s, and an output is produced every 0.5 s, i.e., the time segments have a 50% overlap. A baseline is computed and removed from the EMG signal according to

$$EMG_c = \begin{cases} EMG - baseline, & \text{if } EMG > baseline \\ 0, & \text{if } EMG \leq baseline \end{cases} \qquad (3)$$

To obtain the baseline, the user must keep his hand in the resting position for one second. During this period, an

algorithm finds 100 peaks in the EMG signal, and then the baseline is obtained from the average of the positive peaks

$$baseline = \frac{1}{N}\sum_{n=0}^{N-1} Peaks[n]\,, \tag{4}$$

where *N=100*. The muscular activity is detected using the RMS (root mean square) of the EMG signal. This method was selected among several others because it was the most effective during experiments and also one of the most used in the literature [8]. The RMS is given by

$$RMS_{EMG} = \sqrt{\frac{1}{S}\sum_{i=0}^{S-1} x_i^2} \tag{5}$$

where x_i is a time sample of the EMG window and S is the number of samples of the window. To detect the movement intention, it is first required to obtain the maximum voluntary contraction (MVC) for each muscle. During a 10 s period, the user is asked to exert his maximum opening/closing contraction. MVC is then given by

$$MVC = \frac{1}{M}\sum_{j=0}^{M-1} RMS_{EMG}(j) \tag{6}$$

where M is the number of windows, set to 20. To detect the movement intention, the features are extracted from both muscles. A threshold is applied to the MVC. If the RMS_{EMG} is higher than this value, a muscular intention is considered, otherwise the muscular activity is not considered, according to

$$RMS_{EMG\_o} = \begin{cases} RMS_{EMG}, & RMS_{EMG} > MVC_{rms} \times thr \\ 0, & RMS_{EMG} \leq MVC_{rms} \times thr \end{cases} \tag{7}$$

where *thr* is a value between 0% and 100% of the MVC for each muscle. The detection of open/close movements is obtained applying the following rules

$$movement = \begin{cases} open\text{: if } RMS_{EMG\_Ext} > RMS_{EMG\ Flex} \\ close\text{: if } RMS_{EMG\_Flex} > RMS_{EMG\ Ext} \\ rest\text{: otherwise} \end{cases} \tag{8}$$

where the RMS_{EMG_Ext} and RMS_{EMG_Flex} are respectively the flexor and extensor RMS values obtained after baseline correction.

III. 3D MODELLING OF HAND EXOSKELETON

The exoskeleton went through several versions to fit the needs of the hand of the hemiplegic participant. Some desired features were: 1) a neutral position relative to prone-supination (forearm movement), with some degree of flexion of the wrist; and 2) movement of the thumb in its two joints (interphalangeal and metacarpophalangeal). Additionally, the high spasticity of the user's hand required high resistance in the orthosis joints. Given all these specificities, we decided to design a 3D exoskeleton fully customized to the hemiplegic participant's hand, which is here described and is still an ongoing work. The exoskeleton is based on phalanges, joints, back of the hand and wrist. The process of modelling the exoskeleton is summarized in Fig. 4. The first step was to obtain a 3D model of the hand, using the depth sensors of the

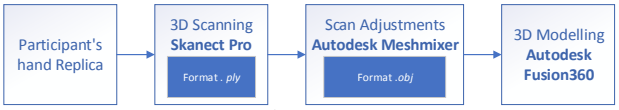

Figure 4. Process of 3D exoskeleton modelling.

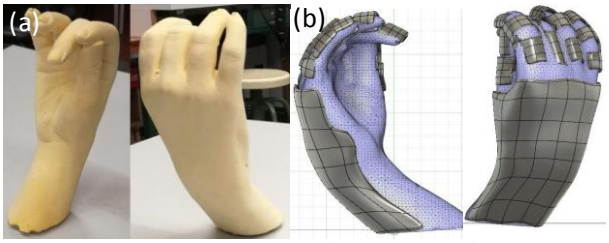

Figure 5. a) Various perspectives of plaster cast performed with Skanect software; b) Digital model made from participant's hand.

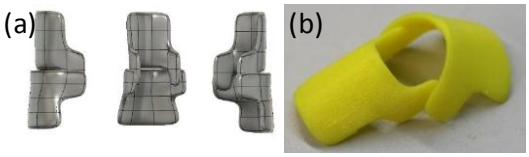

Figure 6. Detail view of: a) 3D model, and b) 3D print of thumb.

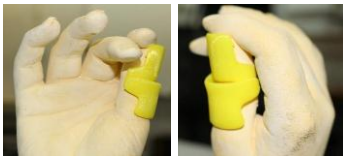
Figure 7. Thumb components placed on participant's hand mold.

Xbox 360 Kinect camera, and Skanect Pro software acting as a 3D scanner. To allow proper scanning, the arm and hand needed to be immobilized. Due to the difficulty of doing a direct scanning, a plaster cast of the hand was made (see Fig. 5a)). The 3D model was then worked on Autodesk Meshmixer software to clean and repair 3D scanning, eliminating noise inherent to the scanning process. Finally, the exoskeleton was modelled using Autodesk Fusion 360. Figure 5b) presents the exoskeleton model fitted to participant's hand. The parts were printed in a 3D printer (Sigma, BCN3D) with PLA (Polylactic Acid) biodegradable, which makes it highly attractive for biological and medical applications [9]. Figure 6a) shows the model made for the thumb finger and Fig. 6b) shows a 3D printed part for the same finger. Fig. 7 shows the thumb parts installed on thumb of the plaster cast.

IV. RESULTS

The current ARHO prototype is based on a non-customized exoskeleton. This version and other exoskeleton versions were tested on the hemiplegic participant, but they did not show the required strength/robustness due to the severe spasticity of his hand and wrist after closing the hand. The customized exoskeleton described in section III is currently being designed to offer the required strength and ergonomics. Therefore, the experiments with the mechanical orthosis were conducted only with healthy participants using a non-customized exoskeleton.

A. Intention detection based on EMG

Before being used, ARHO needs a calibration procedure to identify the baseline and to obtain the MVC, a process that

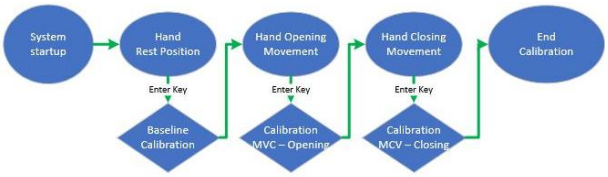

Figure 8. Flowchart of ARHO calibration.

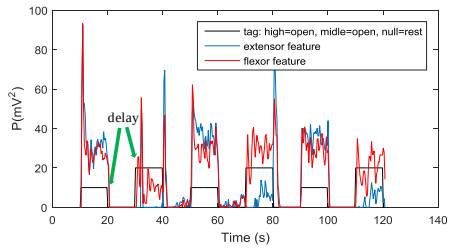

Figure 9. RMS feature extraction of flexor and extensor muscles for different movements of one healthy participant

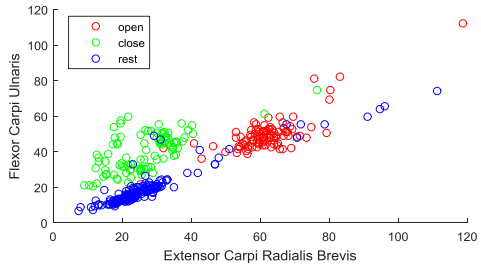

Figure 10. Scatter plot flexor vs extensor for the same data of Fig. 9.

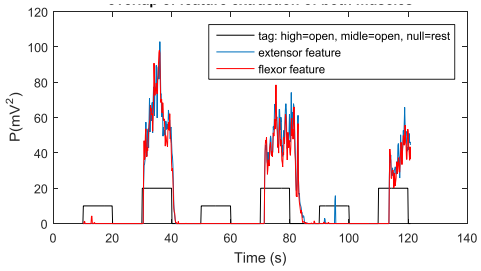

Figure 11. RMS feature extraction of both muscles of the hemiplegic participant.

takes about 20 s (Fig. 8). Experiments to assess the detection of user intent based on EMG were performed in 3 healthy participants and in the hemiplegic participant. Figure 9 shows the extracted features in the flexor and extensor muscles for successive movements of opening and closing with resting in between, made by one healthy participant. Baseline and RMS feature extraction seem effective for the identification of the 3 classes. This is emphasized in the scatterplot shown in Fig. 10, which shows that each movement appears in distinct areas. The occurrence of most outliers is explained by the buffering delay which induces wrong classifications during movement transitions, i.e., due to the delay between the classification and the instruction cue/tag (see Fig. 9). The EMG experiments performed with the hemiplegic participant show that the muscular activity of his affected forearm is not detectable, as observed in Fig. 11, and therefore impossible to use for intention detection. Still, this participant can use the system manually triggering the open/close movement with the non-affected hand, or mimicking the non-affected hand. Other muscles of the upper arm of the affected side are also being considered. One healthy participant, with the approximate hand size of the hemiplegic participant, was asked to perform grasping movements with ARHO. The experiment consisted in 20 grasping movements (closing, resting and opening movements). The task was performed in a controlled environment, and the participant was seated in a resting position. Table I shows the confusion matrix for the 3 classes. The classification performance was respectively 91%, 96% and 97% and the overall classification accuracy was 95%. The results show the effectiveness of the signal processing and classification methods and of the grasping functionality.

Despite the encouraging results, there are several limitations of the current ARHO mechanical prototype with regard to strength, ergonomics, extension of movements, general usability, and aesthetics. The ongoing 3D model of the exoskeleton customized to the hemiplegic participant is expected to provide a significant improvement regarding these issues. However, the size and weight (380g) of ARHO should also be improved. As additional features, one of the most important would be the integration of force sensors in the finger tips to have force feedback to grab objects of different sizes.

TABLE I. ONLINE PERFORMANCE FOR GRASPING TASKS (3 CLASSES)

	detected movement			
order	open	close	rest	success
open	154	3	11	91%
close	1	247	9	96%
rest	7	0	231	97%

V. REFERENCIES

[1] E. Susanto, R. K. Tong, C. Ockenfeld and N. SK Ho, "Efficacy of robot-assisted fingers training in chronic stroke survivors: a pilot randomized-controlled trial," *J. of NeuroEng. and Rehab.*, vol. 12, 2015.

[2] P. Heo, G. M. Gu, S.-j. Lee, K. Rhee e J. Kim, "Current Hand Exoskeleton Technologies for Rehabilitation and Assistive Engineering," *Int. J. of Precision Eng. & Manuf.* , vol. 13, May 2012.

[3] R. A. Bos, C. J. Haarman, T. Stortelde, K. Nizamis, J. L. Herder, A. H. Stienen e D. H. Plettenburg, "A structured overview of trends and technologies used in dynamic hand orthoses," *Journal of NeuroEngineering and Rehabilitation*, vol. 13:62, 2016.

[4] A. Chiri, N. Vitiello, F. Giovacchini, S. Roccella, F. Vecchi e M. C. Carrozza, "Mechatronic Design and Characterization of the Index Finger Module of a Hand Exoskeleton for Post-Stroke Rehabilitation," *IEEE/ASME Trans. on Mechatr.*, vol. 17, 2012.

[5] J. Christopher, B. Tobias, L. Olivier, A. Jumpei, G. Fischer and R. Gassert, "Design and Characterization of a Lightweight and Fully Portable Remote Actuation System for Use With a Hand Exoskeleton," *IEEE Rob. and Aut. Lett.*, vol. 1, 2016.

[6] H. In, B. B. Kang, M. Sin and a. K.-J. Cho, "Exo-Glove: A Soft Wearable Robot for the Hand with a Soft Tendon Routing System," *IEEE Rob. & Autom. Magazine* , vol. 22, March 2015.

[7] A. M. Devices, "Actuonix Motion Devices," [Online]. Available: https://www.actuonix.com/L16-Linear-Actuators-p/l16-p.htm.

[8] M. Hakonena, H. Piitulainen and A. Visala, "Current state of digital signal processing in myoelectric interfaces and related applications," *Biom. Signal Process. and Control*, vol. 18, 2015.

[9] J. Hilborn, N. Revagade e B. Gupta, "Science Direct," *Poly(lactic acid) fiber: An overview*, pp. 455-482, April 2007.